Appl Phys A (2013) 112:241–254
DOI 10.1007/s00339-013-7658-7

Applied Physics A
Materials Science & Processing

INVITED PAPER

A perspective of recent progress in ZnO diluted magnetic semiconductors

Zheng Yang

Received: 10 September 2012 / Accepted: 5 March 2013 / Published online: 11 May 2013
© Springer-Verlag Berlin Heidelberg 2013

Abstract ZnO has long been considered as a promising candidate material for diluted magnetic semiconductors, owing to its theoretically predicted and experimentally observed above-room-temperature ferromagnetism and long spin-coherence time. In this brief perspective, recent progress in ZnO diluted magnetic semiconductors is reviewed with particular focus on three topics: (1) spin coherence in ZnO; (2) free-carrier type and concentration-dependent magnetic properties in ZnO; and (3) ferromagnetism in undoped and non-transition-metal-doped ZnO. Finally, current status and possible potential direction of research on ZnO diluted magnetic semiconductors are summarized in the concluding remarks.

1 Introduction

Diluted magnetic semiconductor (DMS) materials have attracted much attention arising from the feasibility of manipulation of both charge and spin degree of freedoms in a single material system [1–4]. Electronic devices employed for data processing in computers such as field-effect transistors in central processing units are made from semiconductor materials; while the memory devices employed for non-volatile data storage in computers such as hard drives are generally made from ferromagnetic materials. Diluted magnetic semiconductor is a kind of material with promising properties of both semiconductors (with a tunable conductance under gate bias) for logic computation and ferromagnetic materials (with a controllable spin polarization) for information storage. With this motivation, research on DMS materials nowadays has become one of the major areas of spintronics [5–8].

Two main factors limit DMS practical applications for devices. One is the Curie temperature of the DMS material; the other is whether the ferromagnetism in the DMS material originates from free-carrier mediation (sometimes referred to as 'intrinsic') or purely from localized secondary phases of magnetic dopants such as clusters or precipitates (sometimes referred to as 'extrinsic'). If the ferromagnetism is not mediated by free carriers, the spin polarization cannot be carried by the free carriers; hence, it is generally not applicable for spintronic devices. The carrier-mediated ferromagnetism has been confirmed in several well-known 'canonical' DMS materials, such as Mn-doped GaAs (GaAs:Mn) [9, 10] and Mn-doped InAs (InAs:Mn) [11, 12], however, all these materials show Curie temperatures far below room temperature. On the other hand, above-room-temperature Curie temperatures have been observed in some DMS materials but the origin of the ferromagnetism is still controversial, especially in oxides and nitrides. ZnO is one of this type of DMS materials.

ZnO is a wide bandgap semiconductor material with a direct bandgap of ∼3.37 eV at room temperature [13], which has promising applications for optoelectronic devices [14] due to its large exciton binding energy (∼60 meV) and direct bandgap [15]. ZnO has attracted lots of interest for DMS research initially due to its predicted above-room-temperature Curie temperature based on theoretical calculations [16–18]. Starting from near the end of the last century growing efforts have been focused on ZnO DMS research and above-room-temperature ferromagnetism in ZnO DMS has been widely observed in experiments [19–56]. Up to the present more than 1300 papers have been published in the ZnO DMS area according to ISI-Web-of-Knowledge statistics. However, the

Z. Yang (✉)
Department of Electrical and Computer Engineering, University of Illinois at Chicago, Chicago, IL 60607, USA
e-mail: yangzhen@uic.edu

origin and mechanism of the ferromagnetism in ZnO DMS are still under intense debate. Recently, the research on ZnO DMS has been primarily focused on the study for clarifying the origin and mechanism of the ferromagnetism in ZnO DMS.

Since the discovery of room-temperature ferromagnetism in ZnO, quite a few review papers have been published on ZnO DMS and other diluted magnetic oxides [4, 57–70]. Compared to previously published comprehensive reviews on ZnO DMS, this brief perspective paper does not go through details on all the aspects in the ZnO DMS area (such as different preparation techniques, growth parameters, transition-metal dopants, etc.), but focuses primarily on the recent progress on three topics: (1) spin coherence in ZnO, (2) free-carrier type and concentration-dependent magnetic properties in ZnO DMS, and (3) ferromagnetism in undoped and non-transition-metal-doped ZnO. The three topics are important for ZnO DMS research. Spin coherence is a critical physical parameter for ZnO DMS device applications. The latter two help to further clarify the origin and mechanism of the ferromagnetic ordering in ZnO DMS and facilitate future development of precisely controllable ZnO DMS.

2 Spin coherence in ZnO

Practical spintronic devices require a long spin-coherence time in the hosting material at room temperature. ZnO material has a wide bandgap and a weak spin–orbit coupling [71], which is likely to lead to a long spin-coherence time. Compared to the large number of publications on ZnO DMS (>1300 papers), the number of publications on spin-coherence study in ZnO is not much (<40 papers), but in recent years it has increased a lot in both experiments [72–84] and theory [85–87]. The representative experimental results of spin coherence in ZnO are summarized in Table 1.

The seminal work on spin-coherence study in ZnO was done by Ghosh et al. using time-resolved Faraday rotation (TRFR) spectroscopy [72]. Spin-coherence times of 20 ns at 30 K in ZnO bulk single crystals and 2 ns at 10 K and ∼188 ps at 280 K in pulsed laser deposition (PLD) grown thin films were observed. Previously, the spin coherence could only be observed and investigated in high-quality ZnO materials such as ZnO bulk single crystals [72, 77, 81] and epitaxial ZnO thin films growth by molecular-beam epitaxy (MBE) and PLD [72, 75, 77]. Recently, the spin coherence has also been successfully studied in ZnO nanoparticles/quantum dots [73, 76, 78–80], spin-coated sol–gel ZnO thin films [82], and ZnO DMS materials doped with Co and Mn [80, 82]. Figure 1a shows the TRFR spectroscopy of spin-coated sol–gel ZnO thin films at 300 K and 10 K. The measurements were performed at a magnetic field of 1.4 T

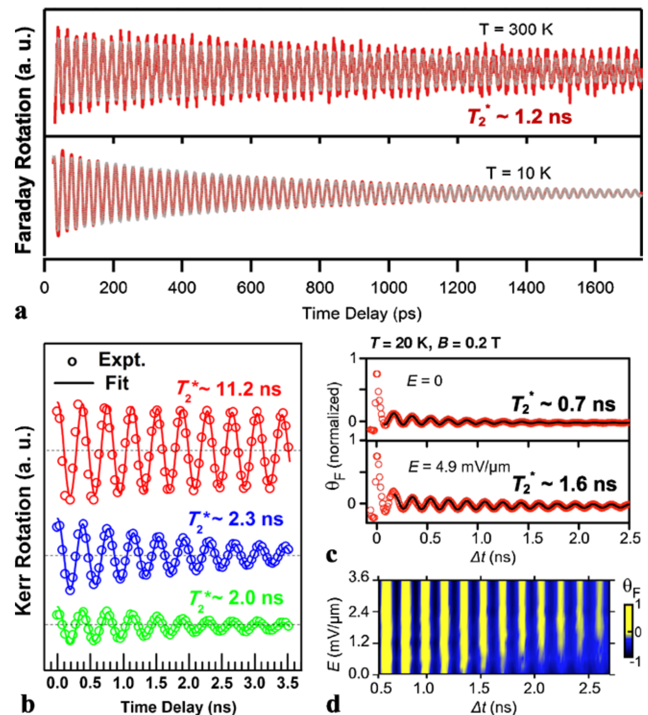

Fig. 1 *Spin-coherence in ZnO*. (**a**) Spin coherence of spin-coated sol–gel ZnO thin films. Time-resolved Faraday rotation spectroscopy of the ZnO thin film at 300 K and 10 K with a magnetic field of 1.4 T. The *red solid lines* and *gray dotted lines* show the experimental data and the exponentially damped sinusoidal fits, respectively. The spin–coherence time is ∼1.2 ns at 300 K. (**b**) Annealing effect on spin coherence of ZnO. Time-resolved Kerr rotation spectroscopy of ZnO single crystal (*top*, *red*) and after rapid thermal annealing in N_2 ambient at 500 °C (*middle*, *blue*) and 800 °C (*bottom*, *green*). The measurements were performed at 8.5 K with a magnetic field of 90 mT. The *circles* and *solid lines* show the experimental data and the exponentially damped sinusoidal fits, respectively. The spin-coherence times are ∼11.2 ns, ∼2.3 ns, and ∼2.0 ns for the ZnO before and after 500 and 800 °C annealing, respectively. (**c**), (**d**) Electric field effect on spin coherence of ZnO. Time-resolved Faraday rotation spectroscopy of epitaxial ZnO thin films (**c**) without (*top*) or with an in-plane electric field of 4.9 mV/μm (*bottom*) and (**d**) at different electric fields of 0–3.6 mV/μm. All the measurements were performed at 20 K with a magnetic field of 0.2 T. The spin-coherence time is enhanced from ∼0.7 ns at zero field to ∼1.6 ns with an electric field of 4.9 mV/μm. [(**a**) reprinted with permission from Ref. [82]. Copyright the American Chemical Society. (**b**) reprinted with permission from Ref. [81]; (**c**)–(**d**) reprinted with permission from Ref. [75]. Copyright the American Institute of Physics]

with laser wavelengths of 375 nm (at 300 K) and 368 nm (at 10 K) [82]. The red solid lines and gray dotted lines show the experimental data and the exponentially damped sinusoidal fits, respectively. The spin-coherence time of the spin-coated ZnO thin film is estimated to be ∼1.2 ns at 300 K. Most of the spin dynamics studies have been focused on the electrons in ZnO. Several studies on the hole [77, 84] and exciton [84] spin dynamics have also been reported.

The spin-coherence property of ZnO can be modified by thermal processing and tuned with external applied bias.

Table 1 Experimental studies of spin coherence in ZnO

Material	Type of spin lifetime	Spin lifetime	Temperature	Method	Note	Reference (year)
ZnO bulk single crystal	Electron spin-coherence time, T_2^*	20 ns	30 K	TRFR	ZnO was grown by HT method	[72] (2005)
ZnO epitaxial thin film grown by PLD	Electron spin-coherence time, T_2^*	2 ns	10 K	TRFR		[72] (2005)
		188 ps	280 K			
ZnO quantum dots	Ensemble spin-dephasing time, T_2^*	25 ns	298 K	EPR		[73] (2007)
CdZnO thin film	Carrier/exciton spin-relaxation time, τ_s	45–60 ps	2 K	TRPPL	The thin films were epitaxially grown by MBE	[74] (2008)
MgZnO thin film		50 ps				
ZnO thin film		80 ps				
ZnO:Ga epitaxial thin film grown by MBE	Electron spin-coherence time, T_2^*	~0.7 ns	20 K	TRFR	No electric field	[75] (2008)*
		~1.6 ns			4.9 mV/μm electric field	
ZnO quantum dots	Electron spin-coherence time, T_2^*	~1.2 ns	10 K	TRFR		[76] (2008)
ZnO epitaxial thin film grown by MBE	Hole spin-relaxation time, T_1	~350 ps	16 K	TRPL		[77] (2009)
	Hole spin-coherence time, T_2	100–350 ps	16 K			
ZnO bulk single crystal	Hole spin-relaxation time, T_1	~100 ps	1.7 K	TRPL		[77] (2009)
	Hole spin-coherence time, T_2	80–100 ps	1.7 K			
ZnO nanocrystals	Ensemble spin-dephasing time, T_2^*	15 ns	RT	EPR		[78] (2010)
	Spin–spin relaxation time, T_2	48.6 ns				
ZnO nanocrystals doped with [^{67}Zn]	Spin–spin relaxation time, T_2	87 ns	RT	EPR	With 0.03 % [^{67}Zn]	[78] (2010)
		40 ns			With 4.1 % [^{67}Zn]	
		24 ns			With 9.6 % [^{67}Zn]	
ZnO nanoparticles	Exciton spin-relaxation time	>1 ns	10 K	TRPPL		[79] (2010)
ZnO:Mn quantum dots	Spin-coherence time, T_2	~0.9 μs	5 K	PEPR		[80] (2011)
ZnO bulk single crystal	Electron spin-coherence time, T_2^*	~11 ns	8.5 K	TRKR	ZnO was grown by SCVT method	[81] (2011)
Annealed ZnO bulk single crystal		~2 ns				
ZnO thin film	Electron spin-coherence time, T_2^*	~1.2 ns	298 K	TRFR	The thin films were prepared by sol–gel spin coating	[82] (2011)**
$Co_{0.0006}Zn_{0.9994}O$ thin film		~100 ps				
ZnO thin films grown by PLD	Spin lifetime	2.6 ns	2 K	MR	Spin lifetimes were derived from the analyses of MR results	[88] (2012)
		2.0 ns	10 K			
		31 ps	200 K			

PLD: pulsed laser deposition; *MBE*: molecular beam epitaxy; *HT*: hydrothermal; *SCVT*: seeded chemical vapor transport; *TRFR*: time-resolved Faraday rotation; *TRKR*: time-resolved Kerr rotation; *EPR*: electron paramagnetic resonance; *PEPR*: pulsed *EPR*; *TRPPL*: time-resolved polarized photoluminescence; *RT*: room temperature; *MR*: magnetoresistance

*Spin coherence time is extracted from the black curve in Fig. 2(a) of Ref. [75]

**Spin coherence time is extracted from the red and green curves in Fig. 3(a) of Ref. [82]

Yang et al. reported that the spin coherence in a ZnO single-crystal wafer sample was degraded after a rapid thermal annealing in N_2 ambient [81]. Figure 1b shows the time-resolved Kerr rotation (TRKR) spectroscopy of ZnO single crystal (top, red) and after rapid thermal annealing in N_2 ambient at 500 °C (middle, blue) and 800 °C (bottom, green). The measurements were performed at 8.5 K with a magnetic field of 90 mT. The open circles and solid lines show the experimental data and the exponentially damped sinusoidal fits, respectively. The spin-coherence times are ∼11.2 ns, ∼2.3 ns, and ∼2.0 ns for the ZnO before and after 500 and 800 °C annealing, respectively. The degraded spin-coherence time is attributed to the annealing-induced surface conducting layer [81]. Ghosh et al. reported that an in-plane electric could enhance the spin coherence in ZnO [75]. Figure 1c shows the TRFR spectroscopy of epitaxial ZnO thin films without (top) and with an in-plane electric field of 4.9 mV/μm (bottom). The spin-coherence time is enhanced from ∼0.7 ns at zero field to ∼1.6 ns with an electric field of 4.9 mV/μm. Figure 1d shows the TRFR mapping at different electric fields of 0–3.6 mV/μm. Both the measurements in Figs. 1c and d were performed at 20 K with a magnetic field of 0.2 T. The capability to electrically manipulate spin coherence is promising. ZnO spin lifetime was also analyzed based on a magnetic tunnel junction device with ZnO as the spacer layer [88].

3 Free-carrier type and concentration-dependent magnetic properties in ZnO

Whether the magnetic properties (e.g. magnetization, Curie temperature, anomalous Hall effect, etc.) of a DMS material show free carrier concentration dependent behavior is an important and straightforward approach to study the origin and mechanism of the ferromagnetism in the DMS. Clear carrier concentration dependent magnetic properties have been demonstrated in 'canonical' DMS materials such as GaAs:Mn and InAs:Mn [9–12], while in other DMS materials it is still controversial, for example nitride and oxide DMS. In recent years, preliminary results of carrier concentration dependent magnetic properties have been reported in ZnO DMS materials [89–104]. Generally, two approaches are employed for tuning the carrier concentration in a semiconductor, one is chemical doping and the other is electrostatic doping. Both ways have been attempted to tune the carrier concentration in ZnO DMS and study how the magnetic properties behave. Experimental results of carrier concentration dependent ferromagnetism in ZnO DMS materials are summarized in Table 2.

3.1 Chemical doping

Clear carrier concentration dependent magnetization in ZnO DMS was first observed in Co-doped ZnO with a donor co-dopant (for tuning the electron concentration) of Al [91] and Ga [94, 99], and (Mn,Ga) co-doped ZnO [95, 105]. Yang et al. studied the above-room-temperature ferromagnetism in a series of ZnO:(Mn,Ga) [95, 105] and ZnO:(Co,Ga) [94] thin film samples with various free electron carrier concentrations. Figure 2a shows the magnetic field dependent magnetization at 300 K of four ZnO:(Mn,Ga) thin film samples with electron carrier concentration of 1.2×10^{20} cm^{-3} (Mn-A), 4.7×10^{19} cm^{-3} (Mn-B), 8.4×10^{18} cm^{-3} (Mn-C), and 3.5×10^{18} cm^{-3} (Mn-D) [95]. The top and bottom insets show the magnetic field dependent magnetization at 10 K of Mn-A and the temperature-dependent magnetization at 2000 Oe of Mn-A, respectively. Figure 2b shows the relation between the saturated magnetization (M_S) and electron carrier concentration (n) of the four ZnO:(Mn,Ga) thin film samples shown in Fig. 2a. Clear electron carrier concentration dependence of the magnetization is observed [95]. The inset shows the x-ray diffraction (XRD) pattern of a ZnO:(Mn,Ga) thin film. The orientation of the thin film is along $(11\bar{2}0)$ direction with the peak full-width-at-half-maximum (FWHM) of ∼0.29°. Transmission electron microscopy (TEM) studies were performed on a ZnO:(Mn,Ga) thin film sample with no secondary phase observed [105]. Figure 2c shows the TEM studies of a ZnO:(Mn,Ga) thin film sample [105]. Figure 2c (i)–(iii) show the cross-sectional TEM and high-resolution TEM (HRTEM) images near the ZnO:(Mn,Ga)-sapphire substrate interface region, and HRTEM image of the ZnO:(Mn,Ga) thin film, respectively. The top and bottom insets in (iii) show the fast Fourier transform pattern and diffraction pattern of the ZnO:(Mn,Ga) thin film [105]. Figure 2d shows the magnetic field dependent magnetization at 300 K of four ZnO:(Co,Ga) thin film samples with electron carrier concentration of 8.3×10^{19} cm^{-3} (Co-A), 3.6×10^{19} cm^{-3} (Co-B), 4.0×10^{18} cm^{-3} (Co-C), and 1.3×10^{18} cm^{-3} (Co-D) [94]. The top inset shows magnetic field dependent magnetization of sample Co-A at 700 K. The bottom inset shows the temperature-dependent magnetization of sample Co-A at 0.2 T. A high-temperature extrapolation fitting ($M \sim M_0(T_C - T)^{1/2}$) indicates the Curie temperature (T_C) is around 950 K. Figure 2e shows the relation between the saturated magnetization (M_S) versus the electron carrier concentration (n) of the four ZnO:(Co,Ga) thin film samples shown in Fig. 2d. The top and bottom insets show the HRTEM image of a ZnO:(Co,Ga) thin film and the cross-sectional HRTEM image near the ZnO:(Co,Ga)-sapphire substrate interface region [94]. The observed magnetization values are large in the study shown in Figs. 2a and 2d, while comparable and even larger magnetization values in

Table 2 Carrier concentration dependent ferromagnetism in ZnO diluted magnetic semiconductors

Material	Approach of carrier concentration tuning	Carrier concentration range achieved in a series (cm^{-3})	Number of samples/biases in the series	Magnetic measurement type	Measurement temperature	Observation	Reference (year)
ZnO:(Co, Al)	Al n-doping	3.8×10^{17}–2.5×10^{20}	5	Magnetization	RT	The larger concentration, the larger magnetization.	[91] (2007)
ZnO:(Mn, Ga)	Ga n-doping	3.5×10^{18}–1.2×10^{20}	4	Magnetization	300 K	The larger concentration, the larger magnetization.	[95, 105] (2008)
ZnO:Co	Gate bias	$\sim 2 \times 10^{17}$ injected/extracted at ± 10 V	4	Magnetization	RT	At $+10$ V gate bias, the magnetization reaches saturation at ~3 kOe. At -5 V gate bias, the magnetization reaches saturation at ~1.5 kOe.	[92] (2008)
ZnO:(Co, Ga)	Ga n-doping	1.3×10^{18}–8.3×10^{19}	5	Magnetization	300 K	The larger concentration, the larger magnetization.	[94] (2008)
ZnO:(Co, Ga)	Ga n-doping	4.0×10^{19} vs 5.7×10^{20}	2	Magnetization and AHE	300 K	Magnetization: 0.35 vs 0.85 μ_B/Co^{2+}; AHE conductivity: 0.002 vs 0.078 Ω^{-1} m^{-1}.	[99] (2009)
ZnO:(Co, Al)	Gate bias	1.65×10^{20} at no gate bias; N/A under gate biases	3	AHE	4 K and 6 K	Increased AHE signal at +5 MV/cm gate bias; decreased AHE signal at −5 MV/cm.	[98] (2009)
ZnO:Mn	Various growth temperatures (RT–600 °C)	7.78×10^{12}–2.51×10^{18}	4	Magnetization	10 K and 300 K	A strong correlation between effective carrier densities and the ferromagnetism in the samples	[101] (2010)

RT: room temperature; *AHE*: anomalous Hall effect

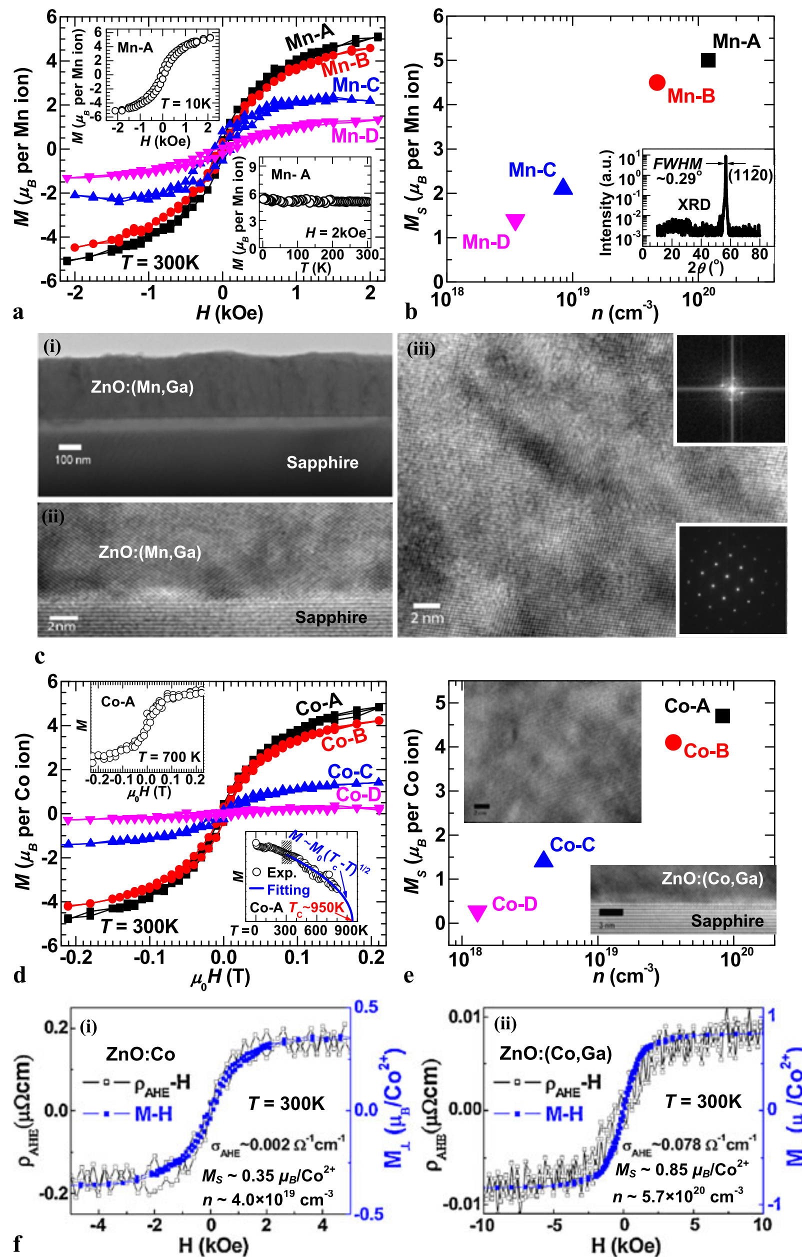

Fig. 2 *Carrier concentration dependent magnetic properties in ZnO DMS thin films*. (**a**) Magnetic field dependent magnetization at 300 K of four ZnO:(Mn,Ga) thin film samples with electron carrier concentration of 1.2×10^{20} cm^{-3} (Mn-A), 4.7×10^{19} cm^{-3} (Mn-B), 8.4×10^{18} cm^{-3} (Mn-C), and 3.5×10^{18} cm^{-3} (Mn-D). *Top inset*: magnetic field dependent magnetization of sample Mn-A at 10 K. *Bottom inset*: temperature-dependent magnetization of sample Mn-A at 2000 Oe. (**b**) The plot of the saturated magnetization (M_S) versus the electron carrier concentration (n) of the four ZnO:(Mn,Ga) thin film samples shown in (**a**). *Inset*: The XRD pattern of a ZnO:(Mn,Ga) thin film. The orientation of the thin film is along (11$\bar{2}$0) direction with a peak FWHM of ~0.29°. (**c**) TEM analyses of a ZnO:(Mn,Ga) thin film sample. (i)–(ii) cross-sectional TEM and HRTEM images near the ZnO:(Mn,Ga)-sapphire substrate interface region, and (iii) HRTEM image of the ZnO:(Mn,Ga) thin film. *Top inset*: fast Fourier transform pattern. *Bottom inset*: diffraction pattern. (**d**) Magnetic field dependent magnetization at 300 K of four ZnO:(Co,Ga) thin film samples with electron carrier concentration of 8.3×10^{19} cm^{-3} (Co-A), 3.6×10^{19} cm^{-3} (Co-B), 4.0×10^{18} cm^{-3} (Co-C), and 1.3×10^{18} cm^{-3} (Co-D). *Top inset*: magnetic field dependent magnetization of sample Co-A at 700 K. *Bottom inset*: temperature-dependent magnetization of sample Co-A at 0.2 T. A high-temperature extrapolation fitting indicates the Curie temperature (T_C) is around 950 K. (**e**) The plot of the saturated magnetization (M_S) versus the electron carrier concentration (n) of the four ZnO:(Co,Ga) thin film samples shown in (**d**). *Top inset*: HRTEM image of a ZnO:(Co,Ga) thin film. The scale bar is 2 nm. *Bottom inset*: cross-sectional HRTEM image near the ZnO:(Co,Ga)-sapphire substrate interface region. The scale bar is 3 nm. (**f**) Magnetic field dependent magnetization (*blue*) and anomalous Hall effect (*black*) in (i) ZnO:Co and (ii) ZnO:(Co,Ga). The ZnO:Co and ZnO:(Co,Ga) thin films show electron concentration (n) of 4.0×10^{19} and 5.7×10^{20} cm^{-3}, saturated magnetization (M_S) of 0.35 and 0.85 μ_B/Co^{2+}, and anomalous Hall conductivity (σ_{AHE}) of 0.002 and 0.078 Ω^{-1} cm^{-1}, respectively. [(**a**)–(**c**) reprinted with permission from Refs. [95, 105]; (**d**)–(**e**) reprinted with permission from Ref. [94]; and (**f**) reprinted with permission from Ref. [99]. Copyright the American Institute of Physics]

ZnO DMS have been reported elsewhere [106, 107]. The free electron concentration dependence of the anomalous Hall effect (AHE) was also observed in ZnO:(Co,Ga) thin films [99]. Figure 2f shows the magnetic field dependent magnetization (blue) and AHE (black) in (i) ZnO:Co and (ii) ZnO:(Co,Ga) thin films. The ZnO:Co and ZnO:(Co,Ga) thin films show electron concentration (n) of 4.0×10^{19} and 5.7×10^{20} cm^{-3}, saturated magnetization (M_S) of 0.35 and 0.85 μ_B/Co^{2+}, and anomalous Hall conductivity (σ_{AHE}) of 0.002 and 0.078 Ω^{-1} cm^{-1}, respectively.

In Dietl's theory [16], ZnO DMS is predicted to have an above-room-temperature Curie temperature when doped with 5 % Mn and within a 3.5×10^{20} cm^{-3} hole concentration p-type environment. In early theoretical work by Sato and Katayama-Yoshida, it was predicted that the ZnO:Mn tends to be ferromagnetic in p-type environment while ZnO:Co tends to be ferromagnetic in n-type environment [17, 108]. Both consistent [42, 47, 51] and inconsistent (ferromagnetic ZnO:Mn in n-type environment) [30, 35, 55] experimental results have been reported. Further efforts need to be focused on ZnO DMS to clarify the carrier type mediation effect.

3.2 Electrostatic doping

Compared to the chemical doping approach, electrostatic doping is a 'cleaner' way to tune the carrier concentration when studying the magnetic properties of DMS materials, due to no additional complexity introduced from the dopants. For example, it has been argued that Ga and Al (donors of ZnO) are likely to introduce additional unknowns to the magnetic properties of ZnO DMS materials because Ga and Al may also form compounds with the magnetic dopants (e.g. Mn, Co, etc.) in addition to their role of tuning electron carrier concentration in ZnO. However, additional fabrication process required for electrostatic doping such as dielectric layer and gate electrode metal deposition takes more effort compared to chemical doping. In ZnO DMSs, only a couple of electrostatic doping studies [92, 98] have been reported so far on investigation of carrier concentration dependent magnetic properties. Gate-bias-dependent magnetization [92] and anomalous Hall effect [98] were reported in ZnO:Co DMS thin films.

4 Ferromagnetism in undoped and non-transition-metal-doped ZnO

Whether the origin of the ferromagnetism is from the secondary phases from the magnetic dopants is a long debate in ZnO DMS. Different from ferromagnetic transition metals Fe, Co, and Ni, transition metals V, Cr, and Mn as well as Ti and Cu do not show any ferromagnetism in their own elemental forms; hence, these transition metals were initially considered as better dopants for ZnO DMS research. However, due to the multi-valence states, ferromagnetism in non-ferromagnetic nanoparticles, or their oxide compounds, recently it has been argued again that dopants V, Cr, Mn, Ti, and Cu in ZnO may introduce complexity and are not ideal dopants when studying the origin and mechanism of the ferromagnetism in ZnO DMS. Recent observations of ferromagnetism in non-transition-metal (e.g., C, Ga, Li, B, etc.)-doped ZnO and undoped ZnO pave an additional way to study the origin and mechanism in ZnO DMS. These results are discussed in this section.

The 'unexpected' magnetism in undoped 'non-magnetic' oxide materials was first observed in HfO_2 thin films by Coey's group [109, 110]. The ferromagnetism was attributed to the defects such as oxygen vacancies. Since then, observation of ferromagnetism has been discovered in various undoped oxide materials, including CeO_2 [111], Al_2O_3 [111], In_2O_3 [111, 112], SnO_2 [111], and TiO_2 [112, 113]. Recently, ferromagnetism has been reported in undoped and non-transition-metal-doped ZnO [100, 111, 114–122] such as C-doped ZnO (ZnO:C) [115, 119], and Ga-doped ZnO (ZnO:Ga) [118]. The representative results of room-temperature ferromagnetism reported in undoped ZnO and non-transition-metal-doped are summarized in Table 3. The origins of the ferromagnetism in these studies are mostly attributed to the intrinsic defects (e.g. oxygen vacancy), defect complex, or mediation of the intrinsic defects in ZnO, except for ZnO:C, in which the origin of ferromagnetism was attributed to Zn–C system [115]. The defect-mediated mechanism of ferromagnetism in ZnO DMSs is different from the carrier-mediation or bound magnetic polaron [45] mechanisms, but it suggests that a precise control of defects in ZnO is also likely to be an alternative approach to design the magnetic properties in ZnO DMSs.

Xu et al. studied the magnetic properties of undoped ZnO thin films [117]. The ZnO thin films were grown on a-plane sapphire substrates using PLD at 570 °C in N_2 ambient under a pressure of 0.3 mbar. The ZnO thin film shows above-room-temperature ferromagnetism. The Curie temperature is above 300 K indicated from the field-cooled and zero-field-cooled curves [117]. Figure 3a (i) shows the magnetic field dependence of the magnetization of the ZnO thin film at 5 K and 290 K with a ferromagnetic hysteresis loop observed at both temperatures. Figure 3a (ii) shows the anomalous Hall resistivity of the ZnO thin film at various temperatures of 5, 20, 50, and 290 K. Two additional interesting observations were reported [117]. First, another undoped ZnO thin film grown at the higher temperature of 655 °C (with all other growth parameters the same) did not show an evident ferromagnetic hysteresis loop, which is attributed to fewer amount of defects in the undoped ZnO at higher temperature. Second, Cu-doped ZnO thin films grown under the

Table 3 Ferromagnetism in undoped and non-transition-metal-doped ZnO diluted magnetic semiconductors

Material	Synthesis method	Curie temperature	Saturated magnetization	AHE	Origin of the ferromagnetism	Note and comment	Reference (year)
ZnO NPs	Sol–gel	≥300 K	~5.0 × 10^{-4} eum/g	N/A	Oxygen vacancies at the surface of the NPs	It was suggested that the ferromagnetism might be a universal characteristic of nanoparticles of metal oxides	[111] (2006)
ZnO thin films	PLD	≥300 K	~200 emu/cm^3	N/A	Defects on Zn sites	Magnetization shows film thickness dependence, indicating that the ferromagnetism likely arises from the defects on thin-film surface and/or at interface of the thin film/substrate	[114] (2007)
ZnO:C thin films	PLD	>400 K	1.5–3.0 μ_B per C	Observed up to 300 K	Zn–C system in the ZnO environment	DFT calculations discussed in the paper predict a magnetic moment of 2.02 μ_B per C atom when C substitutes O in ZnO	[115] (2007)
ZnO powder	Miceller method	~340 K	~0.0018 emu/gm at 300 K	N/A	Magnetic moments can be formed at anionic vacancy clusters	(1) Annealed sample shows stronger magnetization than as-prepared sample. (2) Strong paramagnetic behavior below 10 K was observed, which was attributed to isolated vacancy clusters of F^+ centers	[116] (2007)
ZnO thin films	PLD	>300 K	~1 emu/cm^3	Observed up to 290 K	Intrinsic defects	AHE was observed in both ferromagnetic undoped ZnO and non-ferromagnetic Cu-doped ZnO thin films, indicating that AHE does not uniquely verify intrinsic ferromagnetism	[117] (2008)
ZnO:Ga thin films	PLD	≥300 K	1.5–2.5 × 10^{-4} emu	N/A	Oxygen vacancies that act as F centers	The ferromagnetic behavior is related to the presence of F centers and the high concentration of free carriers	[118] (2008)
ZnO:C thin films	PLD + C implantation	≥300 K	0.24 μ_B per C at 5 K (1 % C)	N/A	C involvement in ZnO	Ferromagnetism was not observed in ZnO, Ne-implanted ZnO, and C-implanted Ge	[119] (2008)
ZnO	PLD	≥300 K	Up to ~1 emu/cm^3	N/A	Defect or defect-complex mediated	Ferromagnetism/diamagnetism can be switched 'Off' and 'On' by employing a high temperature oxygen annealing	[100] (2010)
ZnO:Li thin films	PLD	433–609 K	~1.2 emu/cm^3 at 300 K	N/A	Cation vacancy	Curie temperature depends on Li concentration and growth condition	[132] (2010)
ZnO:B thin films	PLD	>RT	Up to ~1.5 emu/cm^3	N/A	The induced magnetic moment of oxygen atoms in the nearest neighbor sites to B–Zn vacancy pairs	Saturated moment depends on the B concentration	[136] (2010)

AHE: anomalous Hall effect; *NPs*: nanoparticles; *PLD*: pulsed laser deposition; *DFT*: density functional theory; *RT*: room temperature

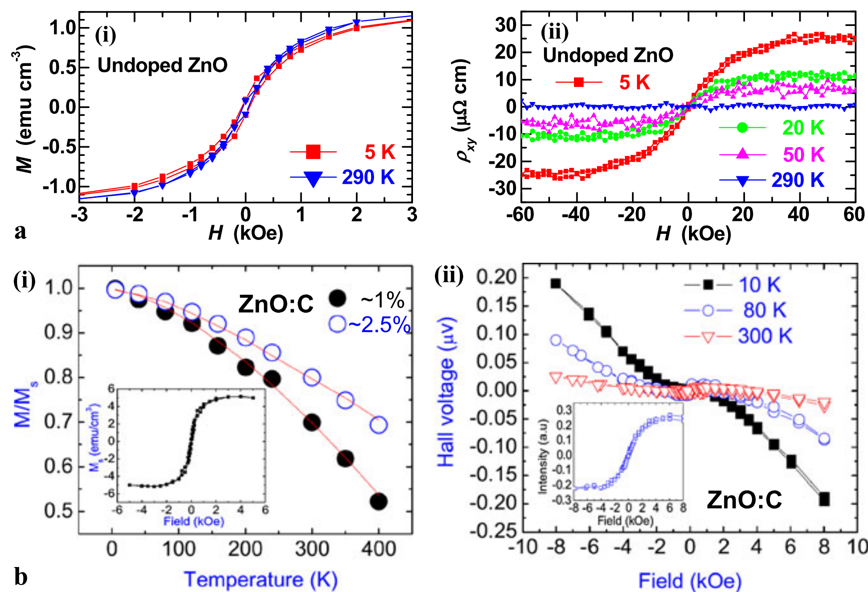

Fig. 3 *Ferromagnetism in transition-metal-free ZnO*. (**a**) Room-temperature ferromagnetism in undoped ZnO thin films. (i) Magnetic field dependence of the magnetization of the ZnO thin film at 5 K and 290 K. Ferromagnetic hysteresis loop observed at both temperatures. (ii) Anomalous Hall resistivity of the ZnO thin film at 5, 20, 50, and 290 K. (**b**) Room-temperature ferromagnetism in ZnO:C thin films. (i) The temperature dependence of the normalized saturation magnetization $[M_S(T)/M_S(5\ \text{K})]$ for ∼1 % (*solid circles*) and ∼2.5 % (*open circles*) ZnO:C thin films. *Inset*: magnetic field dependent magnetization of the ∼1 % ZnO:C thin film at 300 K with a hysteresis loop observed. (ii) Field-dependent Hall effect of the ∼1 % ZnO:C thin film at 10, 80, and 300 K. *Inset*: anomalous Hall effect curve after subtraction of the linear background from the normal Hall effect. [(**a**) reprinted with permission from Ref. [117]. Copyright the American Institute of Physics. (**b**) reprinted with permission from Ref. [115]. Copyright the American Physical Society]

same growth conditions as the ferromagnetic undoped ZnO did not show ferromagnetism in the magnetization measurement; however, they unexpectedly showed an evident AHE in the transport measurements. The authors then concluded that the AHE should not be used as an indication of intrinsic ferromagnetism. The AHE [123] was previously considered as a sign for intrinsic ferromagnetism in ZnO DMS materials [68, 94, 98, 99, 103, 105, 115, 124–131], but now it is more widely accepted that the mechanism of AHE determines whether it is intrinsic (e.g. intrinsic deflection mechanism) or extrinsic (e.g. side jump mechanism, skew scattering mechanism) [123].

Pan et al. studied the magnetic properties of ZnO:C thin films [115]. The ZnO:C thin films were grown on *c*-plane sapphire substrates using PLD at 400 °C and a pressure $<10^{-7}$ torr. The ZnO:C samples show above-room-temperature ferromagnetism. Figure 3b (i) shows the temperature dependence of the normalized saturation magnetization $[M_S(T)/M_S(5\ \text{K})]$ for ∼1 % (solid circles) and ∼2.5 % (open circles) ZnO:C thin films. The inset in Fig. 3b (i) shows the magnetic field dependent magnetization of the ∼1 % ZnO:C thin film at 300 K with a hysteresis loop observed. The Curie temperature is higher than 400 K indicated by the temperature dependent saturation magnetization curve shown in Fig. 3b (i). The undoped ZnO control sample shows non-magnetic properties. In the two ZnO:C samples under study, the larger C concentration sample (∼2.5 % measured by secondary ion mass spectroscopy) shows a stronger magnetization (7.1 emu cm^{-3} at 300 K) than the smaller C concentration sample (∼1 %; 5.1 emu cm^{-3} at 300 K). No ferromagnetism was observed in carbon powder, sintered ZnO/C targets, and the sapphire substrate. The AHE was also observed in the ZnO:C samples with a consistent shape of hysteresis loop with the magnetization hysteresis loop. Figure 3b (ii) shows the field-dependent Hall effect of the ∼1 % ZnO:C sample at 10, 80, and 300 K. The inset in Fig. 3b (ii) shows the AHE curve after the linear background (from the normal Hall effect) was subtracted. Density functional theory (DFT) calculations based on a supercell with 18 f.u. wurtzite ZnO were employed to discuss the experimental results. The magnetism in ZnO:C arises from the carbon substitution for oxygen forming a Zn–C system in the ZnO environment. The magnetic moment is 2.02 μ_B per carbon dopant predicted by the DFT calculation, which is in good agreement with the experiments.

Room-temperature ferromagnetism has also been reported in Li-doped ZnO [49, 132–135] and B-doped ZnO [136, 137], with the origin of the ferromagnetism attributed to the cation vacancy [132] and the induced magnetic moment of oxygen atoms in the nearest-neighbor sites to B–Zn vacancy pairs [136], respectively.

5 Concluding remarks and outlook

Above-room-temperature ferromagnetism has been widely observed and reported in ZnO DMS materials so far. Currently the centerpiece of ZnO DMS research is to further clarify the origin and mechanism of the ferromagnetism in ZnO DMS materials. To investigate the role of free-carrier concentration in the magnetic properties of ZnO DMS materials is an indispensable approach in this direction. Different from the 'canonical' DMS material GaAs:Mn [2, 138] (in which Mn itself is not only a magnetic dopant but an acceptor dopant introducing holes as well), in ZnO DMS materials the magnetic dopants such as Mn and Co do not provide additional electrons or holes in significant amounts, because all the common magnetic dopant elements are generally not shallow donors/acceptors in ZnO at all. Hence, in order to tune the carrier concentration in ZnO DMS using the chemical doping approach, a second dopant element in addition to the magnetic dopant element is required such as Ga [94, 95, 99] and Al [91]; however, the donor/acceptor dopants introduce additional complexity at the same time of supplying free carriers for the mechanism analyses, because the role of the free carriers introduced by the donor/acceptor dopants has to be clearly distinguished from other possible contributions from the donor/acceptor dopants themselves, especially when these dopants compound with magnetic dopants or introduce defects in ZnO showing evident magnetic property changes. For example, ferromagnetism has been reported in ZnO:Ga (without any magnetic dopants) recently [118], as discussed in the previous section. We need to pay additional attention to make a conclusion that the magnetic property is dependent on the free-carrier concentration rather than the concentration of the donor/acceptor dopants. Additionally, to achieve a reliable p-type environment in ZnO with controllable free-hole concentration is also indispensable for the carrier mediation mechanism study of ZnO DMSs, which is still a challenge using the chemical doping method. Most of the free carrier concentration dependent magnetic property studies in ZnO DMSs are under electron environment so far.

Compared to the chemical doping method, electrostatic doping is a 'cleaner' approach to tune the carrier concentration in a semiconductor material controllably with the applied gate voltages. Although preliminary results on carrier concentration dependent magnetization [92] and anomalous Hall effect [98] under electrostatic doping have been reported in ZnO DMS materials, a lot more work still needs to be done to reach solid conclusions comparable to the achievements from similar experiments in 'canonical' DMSs GaAs:Mn [2, 9, 10, 139, 140] and InAs:Mn [11, 12]. Furthermore, how the Curie temperature changes with carrier concentration has not yet been carefully studied in ZnO DMS materials. No experimental results showing a clear conclusion have been reported so far to the best knowledge of the author. These studies under electrostatic doping are important to ZnO DMS research and worthwhile to be focused on in the near future. Recent discovery of the ionic-liquid gating technique [141–146] paves the way for a novel electrostatic doping approach with orders-of-magnitude higher free-carrier concentration achievable than the electrostatic doping using conventional solid gate-dielectrics. Exciting results have been reported in several DMS materials using ionic-liquid gated electrostatic doping recently [144, 145]. Studies on ionic-liquid-gated ZnO DMS devices are likely to further clarify the carrier-mediation mechanism therein due to the opportunity of a larger range of tunable free-carrier concentration.

Finally, it is necessary to point out here that ZnO is a semiconductor material with many species of native defects and impurities with quite a few of them behaving as shallow donors [13, 147, 148]. Quite different from classical semiconductors such as Si and GaAs, ZnO materials prepared using various growth methods from different groups generally show significant differences in physical properties including native defect/impurity species and density, mobility, crystallinity etc. Sometimes the difference could be as large as many orders of magnitude; for example, the electron concentration in undoped ZnO prepared by various methods can range as large as from 10^{15} cm^{-3} to 10^{20} cm^{-3}. When these ZnO materials are employed for DMS study, it is not a surprise that distinct results are reported even with similar magnetic doping conditions. It is a significant difficulty hindering the progress in further clarification of the controversial issues in ZnO DMS research. Once high-quality undoped ZnO materials with low density of native defects and impurities, showing comparable background electron concentration to bulk crystals [149–154], as well as negligible physical property difference from one group to the other within the research community, can be widely prepared in the future, a more reliable platform and basis for ZnO DMS research is established. Research results of ZnO DMS achieved based on this platform can be more reasonably and reliably compared from one group to the other for analyses.

It is still a long way to go with tremendous efforts towards practical device application of the above-room-temperature ferromagnetism demonstrated in ZnO DMS materials, although reported preliminary results of some prototype devices such as ZnO DMS magnetic tunnel junctions [155] have shown promising interest and potential application.

Acknowledgements Financial support from the University of Illinois at Chicago is acknowledged. The author would like to thank Prof. Qingyu Xu (Southeast Univ., China) and Prof. Di Wu (Nanjing Univ., China) for reading the first draft of the manuscript prepared for this review article and Prof. Xu's comments.

References

1. J.K. Furdyna, Diluted magnetic semiconductors. J. Appl. Phys. **64**, R29–R64 (1988)
2. H. Ohno, Making nonmagnetic semiconductors ferromagnetic. Science **281**, 951–956 (1998)
3. A.H. Macdonald, P. Schiffer, N. Samarth, Ferromagnetic semiconductors: moving beyond (Ga,Mn)As. Nat. Mater. **4**, 195–202 (2005)
4. T. Dietl, A ten-year perspective on dilute magnetic semiconductors and oxides. Nat. Mater. **9**, 965–974 (2010)
5. G.A. Prinz, Magnetoelectronics. Science **282**, 1660–1663 (1998)
6. S.A. Wolf, D.D. Awschalom, R.A. Buhrman, J.M. Daughton, S. von Molnar, M.L. Roukes, A.Y. Chtchelkanova, D.M. Treger, Spintronics: a spin-based electronics vision for the future. Science **294**, 1488–1495 (2001)
7. I. Zutic, J. Fabian, S. Das Sarma, Spintronics: fundamentals and applications. Rev. Mod. Phys. **76**, 323–410 (2004)
8. D.D. Awschalom, M.E. Flatte, Challenges for semiconductor spintronics. Nat. Phys. **3**, 153–159 (2007)
9. F. Matsukura, H. Ohno, A. Shen, Y. Sugawara, Transport properties and origin of ferromagnetism in (Ga,Mn)As. Phys. Rev. B **57**, R2037–R2040 (1998)
10. D. Chiba, F. Matsukura, H. Ohno, Electric-field control of ferromagnetism in (Ga,Mn)As. Appl. Phys. Lett. **89**, 162505 (2006)
11. H. Ohno, D. Chiba, F. Matsukura, T. Omiya, E. Abe, T. Dietl, Y. Ohno, K. Ohtani, Electric-field control of ferromagnetism. Nature **408**, 944–946 (2000)
12. D. Chiba, M. Yamanouchi, F. Matsukura, H. Ohno, Electrical manipulation of magnetization reversal in a ferromagnetic semiconductor. Science **301**, 943–945 (2003)
13. U. Ozgur, Y.I. Alivov, C. Liu, A. Teke, M.A. Reshchikov, S. Dogan, V. Avrutin, S.J. Cho, H. Morkoc, A comprehensive review of ZnO materials and devices. J. Appl. Phys. **98**, 041301 (2005)
14. Z. Yang, S. Chu, W.V. Chen, L. Li, J.Y. Kong, J.J. Ren, P.K.L. Yu, J.L. Liu, ZnO:Sb/ZnO:Ga light emitting diode on c-plane sapphire by molecular beam epitaxy. Appl. Phys. Express **3**, 032101 (2010)
15. D.C. Look, Recent advances in ZnO materials and devices. Mater. Sci. Eng. B **80**, 383–387 (2001)
16. T. Dietl, H. Ohno, F. Matsukura, J. Cibert, D. Ferrand, Zener model description of ferromagnetism in zinc-blende magnetic semiconductors. Science **287**, 1019–1022 (2000)
17. K. Sato, H. Katayama-Yoshida, First principles materials design for semiconductor spintronics. Semicond. Sci. Technol. **17**, 367–376 (2002)
18. K. Sato, L. Bergqvist, J. Kudrnovsky, P.H. Dederichs, O. Eriksson, I. Turek, B. Sanyal, G. Bouzerar, H. Katayama-Yoshida, V.A. Dinh, T. Fukushima, H. Kizaki, R. Zeller, First-principles theory of dilute magnetic semiconductors. Rev. Mod. Phys. **82**, 1633–1690 (2010)
19. T. Fukumura, Z.W. Jin, A. Ohtomo, H. Koinuma, M. Kawasaki, An oxide-diluted magnetic semiconductor: Mn-doped ZnO. Appl. Phys. Lett. **75**, 3366–3368 (1999)
20. K. Ando, H. Saito, Z.W. Jin, T. Fukumura, M. Kawasaki, Y. Matsumoto, H. Koinuma, Magneto-optical properties of ZnO-based diluted magnetic semiconductors. J. Appl. Phys. **89**, 7284–7286 (2001)
21. K. Ando, H. Saito, Z.W. Jin, T. Fukumura, M. Kawasaki, Y. Matsumoto, H. Koinuma, Large magneto-optical effect in an oxide diluted magnetic semiconductor $Zn_{1-x}Co_xO$. Appl. Phys. Lett. **78**, 2700–2702 (2001)
22. T. Fukumura, Z.W. Jin, M. Kawasaki, T. Shono, T. Hasegawa, S. Koshihara, H. Koinuma, Magnetic properties of Mn-doped ZnO. Appl. Phys. Lett. **78**, 958–960 (2001)
23. Z.W. Jin, T. Fukumura, M. Kawasaki, K. Ando, H. Saito, T. Sekiguchi, Y.Z. Yoo, M. Murakami, Y. Matsumoto, T. Hasegawa, H. Koinuma, High throughput fabrication of transition-metal-doped epitaxial ZnO thin films: a series of oxide-diluted magnetic semiconductors and their properties. Appl. Phys. Lett. **78**, 3824–3826 (2001)
24. K. Ueda, H. Tabata, T. Kawai, Magnetic and electric properties of transition-metal-doped ZnO films. Appl. Phys. Lett. **79**, 988–990 (2001)
25. J.H. Kim, H. Kim, D. Kim, Y.E. Ihm, W.K. Choo, Magnetic properties of epitaxially grown semiconducting $Zn_{1-x}Co_xO$ thin films by pulsed laser deposition. J. Appl. Phys. **92**, 6066–6071 (2002)
26. K.J. Kim, Y.R. Park, Spectroscopic ellipsometry study of optical transitions in $Zn_{1-x}Co_xO$ alloys. Appl. Phys. Lett. **81**, 1420–1422 (2002)
27. H.J. Lee, S.Y. Jeong, C.R. Cho, C.H. Park, Study of diluted magnetic semiconductor: Co-doped ZnO. Appl. Phys. Lett. **81**, 4020–4022 (2002)
28. Y.Q. Chang, D.B. Wang, X.H. Luo, X.Y. Xu, X.H. Chen, L. Li, C.P. Chen, R.M. Wang, J. Xu, D.P. Yu, Synthesis, optical, and magnetic properties of diluted magnetic semiconductor $Zn_{1-x}Mn_xO$ nanowires via vapor phase growth. Appl. Phys. Lett. **83**, 4020–4022 (2003)
29. D.P. Norton, M.E. Overberg, S.J. Pearton, K. Pruessner, J.D. Budai, L.A. Boatner, M.F. Chisholm, J.S. Lee, Z.G. Khim, Y.D. Park, R.G. Wilson, Ferromagnetism in cobalt-implanted ZnO. Appl. Phys. Lett. **83**, 5488–5490 (2003)
30. D.P. Norton, S.J. Pearton, A.F. Hebard, N. Theodoropoulou, L.A. Boatner, R.G. Wilson, Ferromagnetism in Mn-implanted ZnO:Sn single crystals. Appl. Phys. Lett. **82**, 239–241 (2003)
31. W. Prellier, A. Fouchet, B. Mercey, C. Simon, B. Raveau, Laser ablation of Co: ZnO films deposited from Zn and Co metal targets on (0001) Al_2O_3 substrates. Appl. Phys. Lett. **82**, 3490–3492 (2003)
32. P.V. Radovanovic, D.R. Gamelin, High-temperature ferromagnetism in Ni^{2+}-doped ZnO aggregates prepared from colloidal diluted magnetic semiconductor quantum dots. Phys. Rev. Lett. **91**, 157202 (2003)
33. A.S. Risbud, N.A. Spaldin, Z.Q. Chen, S. Stemmer, R. Seshadri, Magnetism in polycrystalline cobalt-substituted zinc oxide. Phys. Rev. B **68**, 205202 (2003)
34. D.A. Schwartz, N.S. Norberg, Q.P. Nguyen, J.M. Parker, D.R. Gamelin, Magnetic quantum dots: synthesis, spectroscopy, and magnetism of Co^{2+}- and Ni^{2+}-doped ZnO nanocrystals. J. Am. Chem. Soc. **125**, 13205–13218 (2003)
35. P. Sharma, A. Gupta, K.V. Rao, F.J. Owens, R. Sharma, R. Ahuja, J.M.O. Guillen, B. Johansson, G.A. Gehring, Ferromagnetism above room temperature in bulk and transparent thin films of Mn-doped ZnO. Nat. Mater. **2**, 673–677 (2003)
36. N.A. Theodoropoulou, A.F. Hebard, D.P. Norton, J.D. Budai, L.A. Boatner, J.S. Lee, Z.G. Khim, Y.D. Park, M.E. Overberg, S.J. Pearton, R.G. Wilson, Ferromagnetism in Co- and Mn-doped ZnO. Solid-State Electron. **47**, 2231–2235 (2003)
37. S. Kolesnik, B. Dabrowski, J. Mais, Structural and magnetic properties of transition metal substituted ZnO. J. Appl. Phys. **95**, 2582–2586 (2004)
38. D.C. Kundaliya, S.B. Ogale, S.E. Lofland, S. Dhar, C.J. Metting, S.R. Shinde, Z. Ma, B. Varughese, K.V. Ramanujachary, L. Salamanca-Riba, T. Venkatesan, On the origin of high-temperature ferromagnetism in the low-temperature-processed Mn–Zn–O system. Nat. Mater. **3**, 709–714 (2004)
39. N.S. Norberg, K.R. Kittilstved, J.E. Amonette, R.K. Kukkadapu, D.A. Schwartz, D.R. Gamelin, Synthesis of colloidal Mn^{2+}:ZnO quantum dots and high-T_C ferromagnetic nanocrystalline thin films. J. Am. Chem. Soc. **126**, 9387–9398 (2004)

40. J.H. Park, M.G. Kim, H.M. Jang, S. Ryu, Y.M. Kim, Co-metal clustering as the origin of ferromagnetism in Co-doped ZnO thin films. Appl. Phys. Lett. **84**, 1338–1340 (2004)
41. C. Ronning, P.X. Gao, Y. Ding, Z.L. Wang, D. Schwen, Manganese-doped ZnO nanobelts for spintronics. Appl. Phys. Lett. **84**, 783–785 (2004)
42. D.A. Schwartz, D.R. Gamelin, Reversible 300 K ferromagnetic ordering in a diluted magnetic semiconductor. Adv. Mater. **16**, 2115–2119 (2004)
43. M. Venkatesan, C.B. Fitzgerald, J.G. Lunney, J.M.D. Coey, Anisotropic ferromagnetism in substituted zinc oxide. Phys. Rev. Lett. **93**, 177206 (2004)
44. J.M.D. Coey, High-temperature ferromagnetism in dilute magnetic oxides. J. Appl. Phys. **97**, 10D313 (2005)
45. J.M.D. Coey, M. Venkatesan, C.B. Fitzgerald, Donor impurity band exchange in dilute ferromagnetic oxides. Nat. Mater. **4**, 173–179 (2005)
46. N.H. Hong, J. Sakai, N.T. Huong, N. Poirot, A. Ruyter, Role of defects in tuning ferromagnetism in diluted magnetic oxide thin films. Phys. Rev. B **72**, 045336 (2005)
47. K.R. Kittilstved, N.S. Norberg, D.R. Gamelin, Chemical manipulation of high-T_C ferromagnetism in ZnO diluted magnetic semiconductors. Phys. Rev. Lett. **94**, 147209 (2005)
48. C.N.R. Rao, F.L. Deepak, Absence of ferromagnetism in Mn- and Co-doped ZnO. J. Mater. Chem. **15**, 573–578 (2005)
49. M.H.F. Sluiter, Y. Kawazoe, P. Sharma, A. Inoue, A.R. Raju, C. Rout, U.V. Waghmare, First principles based design and experimental evidence for a ZnO-based ferromagnet at room temperature. Phys. Rev. Lett. **94**, 187204 (2005)
50. H.S. Hsu, J.C.A. Huang, Y.H. Huang, Y.F. Liao, M.Z. Lin, C.H. Lee, J.F. Lee, S.F. Chen, L.Y. Lai, C.P. Liu, Evidence of oxygen vacancy enhanced room-temperature ferromagnetism in Co-doped ZnO. Appl. Phys. Lett. **88**, 242507 (2006)
51. K.R. Kittilstved, W.K. Liu, D.R. Gamelin, Electronic structure origins of polarity-dependent high-T_C ferromagnetism in oxide-diluted magnetic semiconductors. Nat. Mater. **5**, 291–297 (2006)
52. K.R. Kittilstved, D.A. Schwartz, A.C. Tuan, S.M. Heald, S.A. Chambers, D.R. Gamelin, Direct kinetic correlation of carriers and ferromagnetism in Co^{2+}: ZnO. Phys. Rev. Lett. **97**, 037203 (2006)
53. T. Andrearczyk, J. Jaroszynski, G. Grabecki, T. Dietl, T. Fukumura, M. Kawasaki, Spin-related magnetoresistance of n-type ZnO:Al and $Zn_{1-x}Mn_xO$:Al thin films. Phys. Rev. B **72**, 121309 (2005)
54. T. Dietl, T. Andrearczyk, A. Lipinska, M. Kiecana, M. Tay, Y.H. Wu, Origin of ferromagnetism in $Zn_{1-x}Co_xO$ from magnetization and spin-dependent magnetoresistance measurements. Phys. Rev. B **76**, 155312 (2007)
55. Y.W. Heo, M.P. Ivill, K. Ip, D.P. Norton, S.J. Pearton, J.G. Kelly, R. Rairigh, A.F. Hebard, T. Steiner, Effects of high-dose Mn implantation into ZnO grown on sapphire. Appl. Phys. Lett. **84**, 2292–2294 (2004)
56. Z. Yang, Z. Zuo, H.M. Zhou, W.P. Beyermann, J.L. Liu, Epitaxial Mn-doped ZnO diluted magnetic semiconductor thin films grown by plasma-assisted molecular-beam epitaxy. J. Cryst. Growth **314**, 97–103 (2011)
57. C. Liu, F. Yun, H. Morkoc, Ferromagnetism of ZnO and GaN: a review. J. Mater. Sci., Mater. Electron. **16**, 555–597 (2005)
58. F. Pan, C. Song, X.J. Liu, Y.C. Yang, F. Zeng, Ferromagnetism and possible application in spintronics of transition-metal-doped ZnO films. Mater. Sci. Eng. R **62**, 1–35 (2008)
59. S.J. Pearton, C.R. Abernathy, D.P. Norton, A.F. Hebard, Y.D. Park, L.A. Boatner, J.D. Budai, Advances in wide bandgap materials for semiconductor spintronics. Mater. Sci. Eng. R **40**, 137–168 (2003)
60. S.J. Pearton, C.R. Abernathy, M.E. Overberg, G.T. Thaler, D.P. Norton, N. Theodoropoulou, A.F. Hebard, Y.D. Park, F. Ren, J. Kim, L.A. Boatner, Wide band gap ferromagnetic semiconductors and oxides. J. Appl. Phys. **93**, 1–13 (2003)
61. W. Prellier, A. Fouchet, B. Mercey, Oxide-diluted magnetic semiconductors: a review of the experimental status. J. Phys. Condens. Matter **15**, R1583–R1601 (2003)
62. S.J. Pearton, W.H. Heo, M. Ivill, D.P. Norton, T. Steiner, Dilute magnetic semiconducting oxides. Semicond. Sci. Technol. **19**, R59–R74 (2004)
63. T. Fukumura, H. Toyosaki, Y. Yamada, Magnetic oxide semiconductors. Semicond. Sci. Technol. **20**, S103–S111 (2005)
64. R. Janisch, P. Gopal, N.A. Spaldin, Transition metal-doped TiO_2 and ZnO—present status of the field. J. Phys. Condens. Matter **17**, R657–R689 (2005)
65. S.A. Chambers, Ferromagnetism in doped thin-film oxide and nitride semiconductors and dielectrics. Surf. Sci. Rep. **61**, 345–381 (2006)
66. S.A. Chambers, T.C. Droubay, C.M. Wang, K.M. Rosso, S.M. Heald, D.A. Schwartz, K.R. Kittilstved, D.R. Gamelin, Ferromagnetism in oxide semiconductors. Mater. Today **9**, 28–35 (2006)
67. J.M.D. Coey, Dilute magnetic oxides. Curr. Opin. Solid State Mater. Sci. **10**, 83–92 (2006)
68. S.J. Pearton, D.P. Norton, M.P. Ivill, A.F. Hebard, J.M. Zavada, W.M. Chen, I.A. Buyanova, ZnO doped with transition metal ions. IEEE Trans. Electron Devices **54**, 1040–1048 (2007)
69. M. Opel, Spintronic oxides grown by laser-MBE. J. Phys. D, Appl. Phys. **45**, 033001 (2012)
70. S.B. Ogale, Dilute doping, defects, and ferromagnetism in metal oxide systems. Adv. Mater. **22**, 3125–3155 (2010)
71. J.Y. Fu, M.W. Wu, Spin-orbit coupling in bulk ZnO and GaN. J. Appl. Phys. **104**, 093712 (2008)
72. S. Ghosh, V. Sih, W.H. Lau, D.D. Awschalom, S.Y. Bae, S. Wang, S. Vaidya, G. Chapline, Room-temperature spin coherence in ZnO. Appl. Phys. Lett. **86**, 232507 (2005)
73. W.K. Liu, K.M. Whitaker, A.L. Smith, K.R. Kittilstved, B.H. Robinson, D.R. Gamelin, Room-temperature electron spin dynamics in free-standing ZnO quantum dots. Phys. Rev. Lett., **98**, 186804 (2007)
74. W.M. Chen, I.A. Buyanova, A. Murayama, T. Furuta, Y. Oka, D.P. Norton, S.J. Pearton, A. Osinsky, J.W. Dong, Dominant factors limiting efficiency of optical spin detection in ZnO-based materials. Appl. Phys. Lett. **92**, 092103 (2008)
75. S. Ghosh, D.W. Steuerman, B. Maertz, K. Ohtani, H. Xu, H. Ohno, D.D. Awschalom, Electrical control of spin coherence in ZnO. Appl. Phys. Lett. **92**, 162109 (2008)
76. N. Janssen, K.M. Whitaker, D.R. Gamelin, R. Bratschitsch, Ultrafast spin dynamics in colloidal ZnO quantum dots. Nano Lett. **8**, 1991–1994 (2008)
77. D. Lagarde, A. Balocchi, P. Renucci, H. Carrere, T. Amand, X. Marie, Z.X. Mei, X.L. Du, Hole spin quantum beats in bulk ZnO. Phys. Rev. B **79**, 045204 (2009)
78. K.M. Whitaker, S.T. Ochsenbein, A.L. Smith, D.C. Echodu, B.H. Robinson, D.R. Gamelin, Hyperfine coupling in colloidal n-type ZnO quantum dots: effects on electron spin relaxation. J. Phys. Chem. C **114**, 14467–14472 (2010)
79. P.M. Chassaing, A. Balocchi, T. Amand, L. Saint-Macary, M.L. Kahn, B. Chaudret, X. Marie, Optical alignment of the exciton in ZnO nanoparticles. Appl. Phys. Lett. **97**, 192112 (2010)
80. S.T. Ochsenbein, D.R. Gamelin, Quantum oscillations in magnetically doped colloidal nanocrystals. Nat. Nanotechnol. **6**, 111–114 (2011)
81. Z. Yang, Y. Li, D.C. Look, H.M. Zhou, W.V. Chen, R.K. Kawakami, P.K.L. Yu, J.L. Liu, Thermal annealing effect on spin coherence in ZnO single crystals. J. Appl. Phys. **110**, 016101 (2011)

82. K.M. Whitaker, M. Raskin, G. Kiliani, K. Beha, S.T. Ochsenbein, N. Janssen, M. Fonin, U. Rudiger, A. Leitenstorfer, D.R. Gamelin, R. Bratschitsch, Spin-on spintronics: ultrafast electron spin dynamics in ZnO and $Zn_{1-x}Co_xO$ sol-gel films. Nano Lett. **11**, 3355–3360 (2011)
83. J. Tribollet, J. Behrends, K. Lips, Ultra long spin coherence time for Fe^{3+} in ZnO: a new spin qubit. Europhys. Lett. **84**, 20009 (2008)
84. D. Lagarde, A. Balocchi, P. Renucci, H. Carrere, F. Zhao, T. Amand, X. Marie, Z.X. Mei, X.L. Du, Q.K. Xue, Exciton and hole spin dynamics in ZnO investigated by time-resolved photoluminescence experiments. Phys. Rev. B **78**, 033203 (2008)
85. N.J. Harmon, W.O. Putikka, R. Joynt, Theory of electron spin relaxation in ZnO. Phys. Rev. B **79**, 115204 (2009)
86. C. Lu, J.L. Cheng, Spin relaxation in n-type ZnO quantum wells. Semicond. Sci. Technol. **24**, 115010 (2009)
87. J. Tribollet, Theory of the electron and nuclear spin coherence times of shallow donor spin qubits in isotopically and chemically purified zinc oxide. Eur. Phys. J. B **72**, 531–540 (2009)
88. M. Althammer, E.M. Karrer-Muller, S.T.B. Goennenwein, M. Opel, R. Gross, Spin transport and spin dephasing in zinc oxide. Appl. Phys. Lett. **101**, 082404 (2012)
89. Z.B. Gu, M.H. Lu, J. Wang, D. Wu, S.T. Zhang, X.K. Meng, Y.Y. Zhu, S.N. Zhu, Y.F. Chen, X.C. Pan, Structure, optical, and magnetic properties of sputtered manganese and nitrogen-Co-doped ZnO films. Appl. Phys. Lett. **88**, 082111 (2006)
90. H. Ndilimabaka, S. Colis, G. Schmerber, D. Muller, J.J. Grob, L. Gravier, C. Jan, E. Beaurepaire, A. Dinia, As-doping effect on magnetic, optical and transport properties of $Zn_{0.9}Co_{0.1}O$ diluted magnetic semiconductor. Chem. Phys. Lett. **421**, 184–188 (2006)
91. X.J. Liu, C. Song, F. Zeng, F. Pan, Enhancement of electrical and ferromagnetic properties by additional Al doping in Co:ZnO thin films. J. Phys. Condens. Matter **19**, 296208 (2007)
92. H. Chou, C.P. Lin, J.C.A. Huang, H.S. Hsu, Magnetic coupling and electric conduction in oxide diluted magnetic semiconductors. Phys. Rev. B **77**, 245210 (2008)
93. G.H. Ji, Z.B. Gu, M.H. Lu, D. Wu, S.T. Zhang, Y.Y. Zhu, S.N. Zhu, Y.F. Chen, Ferromagnetism in Mn and Sb Co-doped ZnO films. J. Phys. Condens. Matter **20**, 425207 (2008)
94. Z. Yang, M. Biasini, W.P. Beyermann, M.B. Katz, O.K. Ezekoye, X.Q. Pan, Y. Pu, J. Shi, Z. Zuo, J.L. Liu, Electron carrier concentration dependent magnetization and transport properties in ZnO:Co diluted magnetic semiconductor thin films. J. Appl. Phys. **104**, 113712 (2008)
95. Z. Yang, J.L. Liu, M. Biasini, P. Beyermann, Electron concentration dependent magnetization and magnetic anisotropy in ZnO:Mn thin films. Appl. Phys. Lett. **92**, 042111 (2008)
96. Y. Belghazi, D. Stoeffler, S. Colis, G. Schmerber, C. Ulhaq-Bouillet, J.L. Rehspringer, A. Berrada, H. Aubriet, J. Petersen, C. Becker, D. Ruch, A. Dinia, Magnetic properties of Al-doped $Zn_{0.95}Co_{0.05}O$ films: experiment and theory. J. Appl. Phys. **105**, 113904 (2009)
97. P. Cao, D.X. Zhao, D.Z. Shen, J.Y. Zhang, Z.Z. Zhang, Y. Bai, Cu^+-codoping inducing the room-temperature magnetism and p-type conductivity of ZnCoO diluted magnetic semiconductor. Appl. Surf. Sci. **255**, 3639–3641 (2009)
98. H.J. Lee, E. Helgren, F. Hellman, Gate-controlled magnetic properties of the magnetic semiconductor (Zn,Co)O. Appl. Phys. Lett. **94**, 212106 (2009)
99. Z.L. Lu, H.S. Hsu, Y.H. Tzeng, J.C.A. Huang, Carrier-mediated ferromagnetism in single crystalline (Co,Ga)-codoped ZnO films. Appl. Phys. Lett. **94**, 152507 (2009)
100. S. Mal, S. Nori, C.M. Jin, J. Narayan, S. Nellutla, A.I. Smirnov, J.T. Prater, Reversible room temperature ferromagnetism in undoped zinc oxide: correlation between defects and physical properties. J. Appl. Phys. **108**, 073510 (2010)
101. D. Mukherjee, T. Dhakal, H. Srikanth, P. Mukherjee, S. Witanachchi, Evidence for carrier-mediated magnetism in Mn-doped ZnO thin films. Phys. Rev. B **81**, 205202 (2010)
102. K. Asano, S. Doi, H. Yamaguchi, T. Komiyama, Y. Chonan, T. Aoyama, Magnetic properties of ZnO:V films formed by pulsed laser deposition with bias voltage application. J. Vac. Sci. Technol. A **29**, 03A119 (2011)
103. X.C. Liu, Z.Z. Chen, E.W. Shi, D.Q. Liao, K.J. Zhou, Room-temperature anomalous Hall effect and magnetoresistance in (Ga,Co)-codoped ZnO diluted magnetic semiconductor films. Chin. Phys. B **20**, 037501 (2011)
104. Y.H. Ye, B. Lu, W.G. Zhang, H.W. Huang, Z.Z. Ye, Study on the structure, optical, electrical and magnetic properties of Mn-Na codoping ZnO nonpolar thin films. Acta Phys. Sin. **61**, 036701 (2012)
105. Z. Yang, W.P. Beyermann, M.B. Katz, O.K. Ezekoye, Z. Zuo, Y. Pu, J. Shi, X.Q. Pan, J.L. Liu, Microstructure and transport properties of ZnO:Mn diluted magnetic semiconductor thin films. J. Appl. Phys. **105**, 053708 (2009)
106. C. Song, K.W. Geng, F. Zeng, X.B. Wang, Y.X. Shen, F. Pan, Y.N. Xie, T. Liu, H.T. Zhou, Z. Fan, Giant magnetic moment in an anomalous ferromagnetic insulator: Co-doped ZnO. Phys. Rev. B **73**, 024405 (2006)
107. A. Zukova, A. Teiserskis, S. van Dijken, Y.K. Gun'ko, V. Kazlauskiene, Giant moment and magnetic anisotropy in Co-doped ZnO films grown by pulse-injection metal organic chemical vapor deposition. Appl. Phys. Lett. **89**, 232503 (2006)
108. K. Sato, H. Katayama-Yoshida, Stabilization of ferromagnetic states by electron doping in Fe-, Co- or Ni-doped ZnO. Jpn. J. Appl. Phys. **40**, L334–L336 (2001)
109. M. Venkatesan, C.B. Fitzgerald, J.M.D. Coey, Unexpected magnetism in a dielectric oxide. Nature **430**, 630 (2004)
110. J.M.D. Coey, M. Venkatesan, P. Stamenov, C.B. Fitzgerald, L.S. Dorneles, Magnetism in hafnium dioxide. Phys. Rev. B **72**, 024450 (2005)
111. A. Sundaresan, R. Bhargavi, N. Rangarajan, U. Siddesh, C.N.R. Rao, Ferromagnetism as a universal feature of nanoparticles of the otherwise nonmagnetic oxides. Phys. Rev. B **74**, 161306 (2006)
112. N.H. Hong, J. Sakai, N. Poirot, V. Brize, Room-temperature ferromagnetism observed in undoped semiconducting and insulating oxide thin films. Phys. Rev. B **73**, 132404 (2006)
113. S.D. Yoon, Y. Chen, A. Yang, T.L. Goodrich, X. Zuo, D.A. Arena, K. Ziemer, C. Vittoria, V.G. Harris, Oxygen-defect-induced magnetism to 880 K in semiconducting anatase TiO_2-delta films. J. Phys. Condens. Matter **18**, L355–L361 (2006)
114. N.H. Hong, J. Sakai, V. Brize, Observation of ferromagnetism at room temperature in ZnO thin films. J. Phys. Condens. Matter **19**, 036219 (2007)
115. H. Pan, J.B. Yi, L. Shen, R.Q. Wu, J.H. Yang, J.Y. Lin, Y.P. Feng, J. Ding, L.H. Van, J.H. Yin, Room-temperature ferromagnetism in carbon-doped ZnO. Phys. Rev. Lett. **99**, 127201 (2007)
116. S. Banerjee, M. Mandal, N. Gayathri, M. Sardar, Enhancement of ferromagnetism upon thermal annealing in pure ZnO. Appl. Phys. Lett. **91**, 182501 (2007)
117. Q.Y. Xu, H. Schmidt, S.Q. Zhou, K. Potzger, M. Helm, H. Hochmuth, M. Lorenz, A. Setzer, P. Esquinazi, C. Meinecke, M. Grundmann, Room temperature ferromagnetism in ZnO films due to defects. Appl. Phys. Lett. **92**, 082508 (2008)
118. V. Bhosle, J. Narayan, Observation of room temperature ferromagnetism in Ga:ZnO: a transition metal free transparent ferromagnetic conductor. Appl. Phys. Lett. **93**, 021912 (2008)
119. S.Q. Zhou, Q.Y. Xu, K. Potzger, G. Talut, R. Grotzschel, J. Fassbender, M. Vinnichenko, J. Grenzer, M. Helm, H. Hochmuth, M. Lorenz, M. Grundmann, H. Schmidt, Room temperature ferromagnetism in carbon-implanted ZnO. Appl. Phys. Lett. **93**, 232507 (2008)

120. C. Guglieri, M.A. Laguna-Marco, M.A. Garcia, N. Carmona, E. Cespedes, M. Garcia-Hernandez, A. Espinosa, J. Chaboy, XMCD proof of ferromagnetic behavior in ZnO nanoparticles. J. Phys. Chem. C **116**, 6608–6614 (2012)
121. X.Y. Xu, C.X. Xu, J. Dai, J.G. Hu, F.J. Li, S. Zhang, Size dependence of defect-induced room temperature ferromagnetism in undoped ZnO nanoparticles. J. Phys. Chem. C **116**, 8813–8818 (2012)
122. Q.Y. Xu, Z. Wen, H. Zhang, X.S. Qi, W. Zhong, L.G. Xu, D. Wu, K. Shen, M.X. Xu, Room temperature ferromagnetism in ZnO prepared by microemulsion. AIP Adv. **1**, 032127 (2011)
123. N. Nagaosa, J. Sinova, S. Onoda, A.H. MacDonald, N.P. Ong, Anomalous Hall effect. Rev. Mod. Phys. **82**, 1539–1592 (2010)
124. Y.Z. Peng, T. Liew, T.C. Chong, C.W. An, W.D. Song, Anomalous Hall effect and origin of magnetism in $Zn_{1-x}Co_xO$ thin films at low Co content. Appl. Phys. Lett. **88**, 192110 (2006)
125. Q.Y. Xu, L. Hartmann, H. Schmidt, H. Hochmuth, M. Lorenz, R. Schmidt-Grund, D. Spemann, M. Grundmann, Magnetoresistance effects in $Zn_{0.90}Co_{0.10}O$ films. J. Appl. Phys. **100**, 013904 (2006)
126. Q.Y. Xu, L. Hartmann, H. Schmidt, H. Hochmuth, M. Lorenz, R. Schmidt-Grund, C. Sturm, D. Spemann, M. Grundmann, Metal-insulator transition in Co-doped ZnO: magnetotransport properties. Phys. Rev. B **73**, 205342 (2006)
127. M. Gacic, G. Jakob, C. Herbort, H. Adrian, T. Tietze, S. Bruck, E. Goering, Magnetism of Co-doped ZnO thin films. Phys. Rev. B **75**, 205206 (2007)
128. Q.Y. Xu, L. Hartmann, H. Schmidt, H. Hochmuth, M. Lorenz, R. Schmidt-Grund, C. Sturm, D. Spemann, M. Grundmann, Y.Z. Liu, Magnetoresistance and anomalous Hall effect in magnetic ZnO films. J. Appl. Phys. **101**, 063918 (2007)
129. Q.Y. Xu, H. Schmidt, L. Hartmann, H. Hochmuth, M. Lorenz, A. Setzer, P. Esquinazi, C. Meinecke, M. Grundmann, Room temperature ferromagnetism in Mn-doped ZnO films mediated by acceptor defects. Appl. Phys. Lett. **91**, 092503 (2007)
130. A.J. Behan, A. Mokhtari, H.J. Blythe, D. Score, X.H. Xu, J.R. Neal, A.M. Fox, G.A. Gehring, Two magnetic regimes in doped ZnO corresponding to a dilute magnetic semiconductor and a dilute magnetic insulator. Phys. Rev. Lett. **100**, 047206 (2008)
131. K. Potzger, S.Q. Zhou, Q.Y. Xu, A. Shalimov, R. Groetzschel, H. Schmidt, A. Mucklich, M. Helm, J. Fassbender, Ferromagnetic structurally disordered ZnO implanted with Co ions. Appl. Phys. Lett. **93**, 232504 (2008)
132. J.B. Yi, C.C. Lim, G.Z. Xing, H.M. Fan, L.H. Van, S.L. Huang, K.S. Yang, X.L. Huang, X.B. Qin, B.Y. Wang, T. Wu, L. Wang, H.T. Zhang, X.Y. Gao, T. Liu, A.T.S. Wee, Y.P. Feng, J. Ding, Ferromagnetism in dilute magnetic semiconductors through defect engineering: Li-doped ZnO. Phys. Rev. Lett. **104**, 137201 (2010)
133. B.Y. Zhang, B. Yao, Y.F. Li, Z.Z. Zhang, B.H. Li, C.X. Shan, D.X. Zhao, D.Z. Shen, Investigation on the formation mechanism of p-type Li-N dual-doped ZnO. Appl. Phys. Lett. **97**, 222101 (2010)
134. B.Y. Zhang, B. Yao, Y.F. Li, A.M. Liu, Z.Z. Zhang, B.H. Li, G.Z. Xing, T. Wu, X.B. Qin, D.X. Zhao, C.X. Shan, D.Z. Shen, Evidence of cation vacancy induced room temperature ferromagnetism in Li-N codoped ZnO thin films. Appl. Phys. Lett. **99**, 182503 (2011)
135. Q.J. Wang, J.B. Wang, X.L. Zhong, Q.H. Tan, Z. Hu, Y.C. Zhou, Magnetism mechanism in ZnO and ZnO doped with nonmagnetic elements X (X = Li, Mg, and Al): A first-principles study. Appl. Phys. Lett. **100**, 132407 (2012)
136. X.G. Xu, H.L. Yang, Y. Wu, D.L. Zhang, S.Z. Wu, J. Miao, Y. Jiang, X.B. Qin, X.Z. Cao, B.Y. Wang, Intrinsic room temperature ferromagnetism in boron-doped ZnO. Appl. Phys. Lett. **97**, 232502 (2010)
137. H.L. Yang, X.G. Xu, X.Y. Zhou, Y.N. Ma, J. Dong, T.Q. Wang, J. Miao, Y. Jiang, Dependence of ferromagnetic properties on growth oxygen partial pressure in boron-doped ZnO thin films. J. Mater. Sci. **47**, 6513–6516 (2012)
138. H. Ohno, A. Shen, F. Matsukura, A. Oiwa, A. Endo, S. Katsumoto, Y. Iye, (Ga,Mn)As: a new diluted magnetic semiconductor based on GaAs. Appl. Phys. Lett. **69**, 363–365 (1996)
139. D. Chiba, A. Werpachowska, M. Endo, Y. Nishitani, F. Matsukura, T. Dietl, H. Ohno, Anomalous Hall effect in field-effect structures of (Ga,Mn)As. Phys. Rev. Lett. **104**, 106601 (2010)
140. M. Sawicki, D. Chiba, A. Korbecka, Y. Nishitani, J.A. Majewski, F. Matsukura, T. Dietl, H. Ohno, Experimental probing of the interplay between ferromagnetism and localization in (Ga,Mn)As. Nat. Phys. **6**, 22–25 (2010)
141. K. Ueno, S. Nakamura, H. Shimotani, A. Ohtomo, N. Kimura, T. Nojima, H. Aoki, Y. Iwasa, M. Kawasaki, Electric-field-induced superconductivity in an insulator. Nat. Mater. **7**, 855–858 (2008)
142. A.T. Bollinger, G. Dubuis, J. Yoon, D. Pavuna, J. Misewich, I. Bozovic, Superconductor-insulator transition in $La_{2-x}Sr_xCuO_4$ at the pair quantum resistance. Nature **472**, 458–460 (2011)
143. M. Weisheit, S. Fahler, A. Marty, Y. Souche, C. Poinsignon, D. Givord, Electric field-induced modification of magnetism in thin-film ferromagnets. Science **315**, 349–351 (2007)
144. Y. Yamada, K. Ueno, T. Fukumura, H.T. Yuan, H. Shimotani, Y. Iwasa, L. Gu, S. Tsukimoto, Y. Ikuhara, M. Kawasaki, Electrically induced ferromagnetism at room temperature in cobalt-doped titanium dioxide. Science **332**, 1065–1067 (2011)
145. M. Endo, D. Chiba, H. Shimotani, F. Matsukura, Y. Iwasa, H. Ohno, Electric double layer transistor with a (Ga,Mn)As channel. Appl. Phys. Lett. **96**, 022515 (2010)
146. Z. Yang, Y. Zhou, S. Ramanathan, Studies on room-temperature electric-field effect in ionic-liquid gated VO_2 three-terminal devices. J. Appl. Phys. **111**, 014506 (2012)
147. A. Janotti, C.G. Van de Walle, Fundamentals of zinc oxide as a semiconductor. Rep. Prog. Phys. **72**, 126501 (2009)
148. M.D. McCluskey, S.J. Jokela, Defects in ZnO. J. Appl. Phys. **106**, 071101 (2009)
149. A. Ohtomo, K. Tamura, K. Saikusa, K. Takahashi, T. Makino, Y. Segawa, H. Koinuma, M. Kawasaki, Single crystalline ZnO films grown on lattice-matched $ScAlMgO_4(0001)$ substrates. Appl. Phys. Lett. **75**, 2635–2637 (1999)
150. A. Tsukazaki, A. Ohtomo, T. Onuma, M. Ohtani, T. Makino, M. Sumiya, K. Ohtani, S.F. Chichibu, S. Fuke, Y. Segawa, H. Ohno, H. Koinuma, M. Kawasaki, Repeated temperature modulation epitaxy for p-type doping and light-emitting diode based on ZnO. Nat. Mater. **4**, 42–46 (2005)
151. A. Tsukazaki, A. Ohtomo, T. Kita, Y. Ohno, H. Ohno, M. Kawasaki, Quantum Hall effect in polar oxide heterostructures. Science **315**, 1388–1391 (2007)
152. A. Tsukazaki, S. Akasaka, K. Nakahara, Y. Ohno, H. Ohno, D. Maryenko, A. Ohtomo, M. Kawasaki, Observation of the fractional quantum Hall effect in an oxide. Nat. Mater. **9**, 889–893 (2010)
153. S. Akasaka, K. Nakahara, A. Tsukazaki, A. Ohtomo, M. Kawasaki, $Mg_xZn_{1-x}O$ films with a low residual donor concentration ($<10^{15}$ cm^{-3}) grown by molecular beam epitaxy. Appl. Phys. Express **3**, 071101 (2010)
154. S. Akasaka, A. Tsukazaki, K. Nakahara, A. Ohtomo, M. Kawasaki, Improvement of electron mobility above 100,000 $cm^2 V^{-1} s^{-1}$ in $Mg_xZn_{1-x}O$/ZnO heterostructures. Jpn. J. Appl. Phys. **50**, 080215 (2011)
155. Q.Y. Xu, L. Hartmann, S.Q. Zhou, A. Mcklich, M. Helm, G. Biehne, H. Hochmuth, M. Lorenz, M. Grundmann, H. Schmidt, Spin manipulation in Co-doped ZnO. Phys. Rev. Lett. **101**, 076601 (2008)